Journal of ELECTRONIC MATERIALS, Vol. 45, No. 9, 2016
DOI: 10.1007/s11664-016-4642-y

Analysis of Etched CdZnTe Substrates

J.D. BENSON,[1,4,5] L.O. BUBULAC,[1] M. JAIME-VASQUEZ,[1] C.M. LENNON,[1] J.M. ARIAS,[1] P.J. SMITH,[1] R.N. JACOBS,[1] J.K. MARKUNAS,[1] L.A. ALMEIDA,[1] A. STOLTZ,[1] P.S. WIJEWARNASURIYA,[2] J. PETERSON,[3] M. REDDY,[3] K. JONES,[3] S.M. JOHNSON,[3] and D.D. LOFGREEN[3]

1.—U. S. Army RDECOM, CERDEC Night Vision and Electronic Sensors Directorate, Ft. Belvoir, USA. 2.—U. S. Army Research Laboratory, Adelphi, USA. 3.—Raytheon Vision Systems, Goleta, USA. 4.—e-mail: david.j.benson@us.army.mil. 5.—e-mail: j.d.benson6.civ@mail.mil

State-of-the-art as-received (112)B CdZnTe substrates have been examined for surface impurity contamination and polishing residue. Two 4 cm × 4 cm and one 6 cm × 6 cm (112)B state-of-the-art as-received CdZnTe wafers were analyzed. A maximum surface impurity concentration of Al = 1.7×10^{15} atoms cm^{-2}, Si = 3.7×10^{13} atoms cm^{-2}, Cl = 3.12×10^{15} atoms cm^{-2}, S = 1.7×10^{14} atoms cm^{-2}, P = 1.1×10^{14} atoms cm^{-2}, Fe = 1.0×10^{13} atoms cm^{-2}, Br = 1.2×10^{14} atoms cm^{-2}, and Cu = 4×10^{12} atoms cm^{-2} was observed on the as-received CdZnTe wafers. CdZnTe particulates and residual SiO_2 polishing grit were observed on the surface of the as-received (112)B CdZnTe substrates. The polishing grit/CdZnTe particulate density on CdZnTe wafers was observed to vary across a 6 cm × 6 cm wafer from ~4×10^7 cm^{-2} to 2.5×10^8 cm^{-2}. The surface impurity and damage layer of the (112)B CdZnTe wafers dictate that a molecular beam epitaxy (MBE) preparation etch is required. The contamination for one 4 cm × 4 cm and one 6 cm × 6 cm CdZnTe wafer after a standard MBE Br:methanol preparation etch procedure was also analyzed. A maximum surface impurity concentration of Al = 2.4×10^{15} atoms cm^{-2}, Si = 4.0×10^{13} atoms cm^{-2}, Cl = 7.5×10^{13} atoms cm^{-2}, S = 4.4×10^{13} atoms cm^{-2}, P = 9.8×10^{13} atoms cm^{-2}, Fe = 1.0×10^{13} atoms cm^{-2}, Br = 2.9×10^{14} atoms cm^{-2}, and Cu = 5.2×10^{12} atoms cm^{-2} was observed on the MBE preparation-etched CdZnTe wafers. The MBE preparation-etched surface contamination consists of Cd(Zn)Te particles/flakes. No residual SiO_2 polishing grit was observed on the (112)B surface.

Key words: CdZnTe substrate, molecular beam epitaxy, polishing damage, impurity contamination

INTRODUCTION

The highest sensitivity, lowest dark current HgCdTe infrared focal-plane arrays (IRFPAs) are currently produced on CdZnTe substrates. A yield-limiting factor in molecular beam epitaxy (MBE) HgCdTe/CdZnTe detector fabrication is presence of macrodefects.[1] Wafer-to-wafer detector variability is also a limiting factor for focal-plane array (FPA) yield. In previous work, two categories of HgCdTe epilayer macrodefects were associated with defects originating from the (112)B CdZnTe substrate surface.[2] Cross-sectional transmission electron microscopy (TEM) analysis traced microvoid defects to pits on the surface of the (112)B CdZnTe substrate.[3] Additional cross-sectional TEM analysis traced morphological defects to raised protrusions on the surface of the (112)B CdZnTe substrate.[2] In both TEM analyses, the defective area was confined to a small region surrounding the CdZnTe pit/protrusion and the HgCdTe epilayer microvoid/morphological defect. This makes the starting CdZnTe as-received surface and substrate preparation extremely critical for high-performance detector fabrication. Last year

(Received January 19, 2016; accepted May 10, 2016; published online June 6, 2016)

we described the initial "out of the box" CdZnTe wafer surface contamination, polishing damage, and Te precipitate size/density in the near-surface region of one 6 cm × 6 cm (112)B state-of-the-art as-received CdZnTe wafer.[4] This year, two additional "out of the box" 4 cm × 4 cm wafers were analyzed. Herein, we also analyze and compare two CdZnTe wafers that have gone through a standard MBE Br:methanol preparation etch. As demonstrated in this paper, impurity contamination and polishing damage exhibit wide lateral variations across a CdZnTe wafer and significant variability wafer to wafer. Our working assumption is that impurity contamination and polishing damage are responsible for many of the large-scale HgCdTe/CdZnTe macrodefects and affect FPA yield. Understanding impurity contamination and polishing damage prior to and after the standard Br:methanol preparation procedure is the first step toward developing a more robust MBE CdZnTe preparation procedure capable of minimizing within-wafer and wafer-to-wafer variability.

EXPERIMENTAL PROCEDURES

Nominal (112)B state-of-the-art CdZnTe substrates were analyzed in this work, specifically 4 cm × 4 cm and 6 cm × 6 cm (112)B state-of-the-art as-received CdZnTe wafers.[4,5] We also used 4 cm × 4 cm and 6 cm × 6 cm (112)B CdZnTe substrates subjected to MBE preparation etch in this work. The ultimate goal of the MBE preparation etch technique is to provide a clean, stoichiometric, atomically smooth, and well-ordered surface to minimize MBE HgCdTe growth defects. Contamination levels and surface damage dictate that the MBE preparation etch needs to remove a damaged surface layer and reduce impurity levels to produce a wafer ready for MBE HgCdTe epitaxial deposition. The current state-of-the-art MBE preparation etch for (112)B CdZnTe used in this work is:[6]

- Organic solvent surface clean (acetone, methanol, isopropanol)
- Br:methanol etch (remove ~5 μm to 10 μm)
- Methanol rinse
- Deionized water rinse

Previous research has shown the MBE preparation etch removes surface damage.[7–9] The Br:methanol MBE preparation etch also leaves a Te-rich surface for initiation of MBE HgCdTe deposition.[10,11]

Nomarski phase-contrast microscopy was used to locate morphological defects on the substrate surface.[12] Atomic force microscopy (AFM) and scanning profilometry were used to characterize surface topography and morphological defects on the CdZnTe substrates. The AFM procedures have been described previously.[12] Scanning electron microscopy (SEM) and energy-dispersive x-ray spectroscopy (EDS) were used to determine the composition of residues found on the (112)B CdZnTe surface and wafer edge.

Total-reflection x-ray fluorescence (TXRF) measurements provided by Evans Analytical Group (EAG)[13] were used to analyze impurities on the surface of 6 cm × 6 cm and 4 cm × 4 cm CdZnTe wafers. TXRF measurements were carried out using a TREX 630T TXRF instrument. The elements Al, Si, P, S, Cl, Cr, Mn, Fe, Ni, Cu, Zn, Ga, Ge, As, Br, Sr, Y, Ta, W, Pt, Au, Hg, Pb, and Bi could be measured using the Mo or W anode configuration to a detection limit of $\sim 1 \times 10^{10}$ atoms cm^{-2}. The analysis spot was a ~10-mm-diameter circle. The analysis depth measured was ~2 nm to 3 nm on the CdZnTe (112)B surface. A square-shaped analysis grid of 25 and 9 locations was measured on the 6 cm × 6 cm and 4 cm × 4 cm samples, respectively. The concentration of impurities was calculated as a uniform contamination layer on the surface in atoms cm^{-2} over the area sampled. Quantification was performed using a Ni-plated Si reference wafer. The reference analysis conditions were corrected for differences between the x-ray optical properties of Si and CdZnTe surfaces. Because the area of the spot analysis is large, particle and macrocontamination within the analysis spot can overestimate the reported surface density measurements.

RESULTS

Impurity Analysis of As-Received CdZnTe Substrates

Last year, we described the initial "out of the box" CdZnTe wafer surface contamination on a 6 cm × 6 cm wafer.[4] This year, two additional "out of the box" 4 cm × 4 cm wafers were analyzed by TXRF. The results from the impurity analysis are presented in Table I. Cr, Mn, Ni, Ga, Ge, As, Sr, Y, Ta, W, Pt, Au, Hg, Pb, and Bi all had maximum concentrations $\leq 1 \times 10^{12}$ atoms cm^{-2} for all three as-received samples measured and are not shown in Table I. Last year, an as-received 6 cm × 6 cm wafer was also characterized by AFM. Numerous particulates were found on the (112)B surface. Particulate length varied from 100 nm to 1 μm. The height of the particulates was measured to be between 10 nm and 300 nm above the (112)B surface. The range of particulate density was 4×10^7 cm^{-2} to 2×10^8 cm^{-2}. In Fig. 1a, a high-resolution SEM/EDS analysis of a "large" particulate on the as-received CdZnTe wafer is shown. The particulate is residual SiO_2 polishing grit. The "large" piece of polishing grit appears to be an agglomeration of smaller pieces of grit. The polishing grit appears to be electrostatically bound to the top surface layer of the CdZnTe, since no binder was found in the EDS analysis shown in Fig. 1a. In Fig. 1b, a high-resolution SEM/EDS analysis of another "large" particulate on a 6 cm × 6 cm as-received CdZnTe wafer is shown. The large

Table I. Results of TXRF analysis on one 6 cm × 6 cm and two 4 cm × 4 cm state-of-the-art as-received (112)B CdZnTe wafers

	Al Atoms (cm^{-2})	Si Atoms (cm^{-2})	P Atoms (cm^{-2})	S Atoms (cm^{-2})	Cl Atoms (cm^{-2})	Fe Atoms (cm^{-2})	Cu Atoms (cm^{-2})	Br Atoms (cm^{-2})	Zn Atoms (cm^{-2})	Particles (cm^{-2})
Maximum density, 6 cm × 6 cm wafer	7.5×10^{14}	3.70×10^{13}	7.10×10^{13}	1.70×10^{14}	3.12×10^{15}	1.02×10^{13}	4.00×10^{12}	1.90×10^{12}	8.00×10^{13}	2.85×10^{8}
Average density, 6 cm × 6 cm wafer	3.7×10^{14}	1.57×10^{13}	4.18×10^{13}	6.69×10^{13}	4.13×10^{14}	7.40×10^{11}	2.19×10^{11}	9.26×10^{11}	4.89×10^{13}	1.41×10^{8}
Coefficient of variation, 6 cm × 6 cm wafer	0.45	0.50	0.31	0.49	1.82	2.68	3.59	0.34	0.23	0.41
Skew, 6 cm × 6 cm wafer	0.88	1.19	0.73	1.85	2.46	4.90	5.00	2.17	1.31	0.79
Maximum density, 4 cm × 4 cm wafer #1	1.70×10^{15}	2.20×10^{13}	9.40×10^{13}	3.90×10^{13}	1.10×10^{14}	5.20×10^{12}	1.00×10^{12}	1.25×10^{14}	2.00×10^{14}	N/A
Average density, 4 cm × 4 cm wafer #1	7.73×10^{14}	1.09×10^{13}	4.60×10^{13}	2.33×10^{13}	7.54×10^{13}	1.60×10^{12}	1.71×10^{11}	1.01×10^{14}	7.64×10^{13}	N/A
Coefficient of variation, 4 cm × 4 cm wafer #1	0.72	0.45	0.44	0.35	0.19	1.06	1.85	0.18	0.85	N/A
Skew, 4 cm × 4 cm wafer #1	1.44	1.84	2.14	1.27	2.47	1.53	2.98	0.56	2.33	N/A
Maximum density, 4 cm × 4 cm wafer #2	7.20×10^{14}	3.30×10^{13}	1.10×10^{14}	5.90×10^{13}	1.60×10^{14}	1.70×10^{12}	9.00×10^{10}	2.20×10^{13}	8.00×10^{13}	N/A
Average density, 4 cm × 4 cm wafer #2	4.37×10^{14}	1.23×10^{13}	5.59×10^{13}	2.51×10^{13}	9.30×10^{13}	6.48×10^{11}	5.13×10^{10}	1.95×10^{13}	5.64×10^{13}	N/A
Coefficient of variation, 4 cm × 4 cm wafer #2	0.29	0.79	0.41	0.56	0.31	0.68	0.36	0.14	0.22	N/A
Skew, 4 cm × 4 cm wafer #2	1.38	1.81	2.19	2.35	2.20	2.24	1.46	−0.52	1.90	N/A

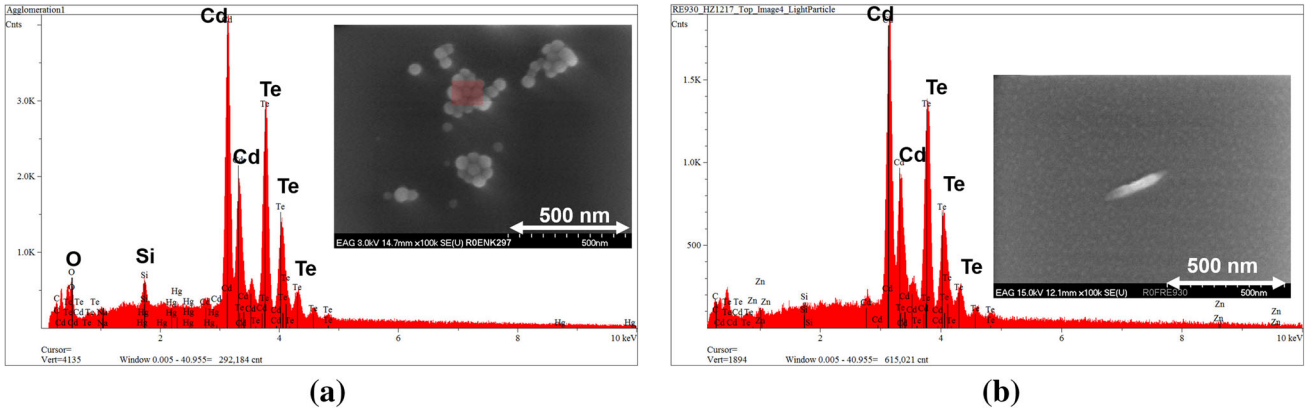

Fig. 1. High-resolution SEM/EDS image analysis of as-received CdZnTe substrate surface. In (a), one "large" piece of polishing grit residue composed of SiO_2 is shown. In (b), the SEM image shows a flake that EDS determines to be Cd(Zn)Te.

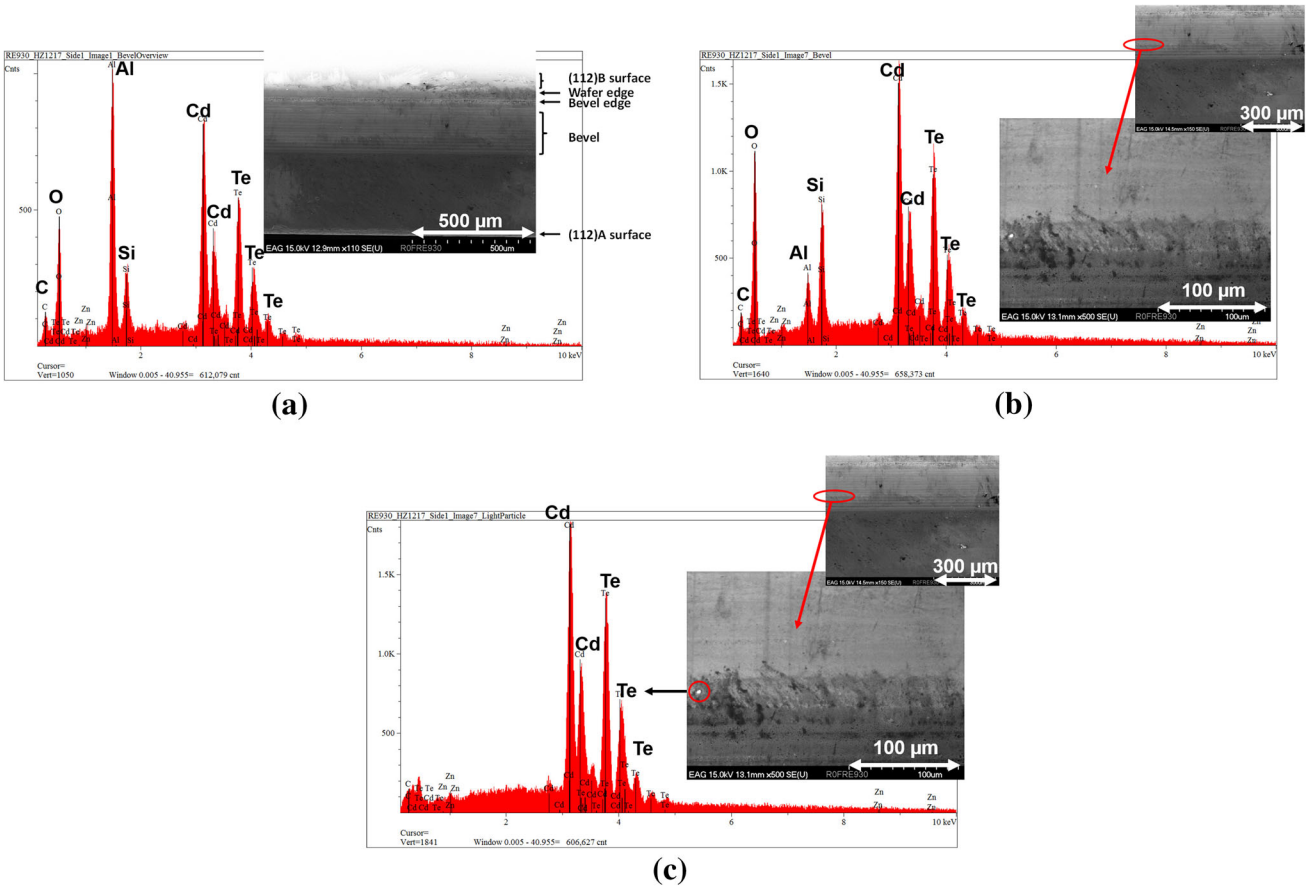

Fig. 2. SEM/EDS image analysis of edge of 6 cm × 6 cm CdZnTe wafer: (a) low-resolution image showing the wafer edge is contaminated with residual SiO_2 (and potentially Al_2O_3) polishing grit, as well as residual wax; (b) high-resolution SEM image and corresponding EDS profile of polishing grit and wax left on the wafer edge; (c) high-resolution SEM image and corresponding EDS profile of CdZnTe particle left on the wafer edge.

particulate is a residual Cd(Zn)Te flake. Again, the Cd(Zn)Te particulate appears to be electrostatically bound to the top surface layer of the substrate, since no binder was found in the EDS analysis shown in Fig. 1b. Numerous additional Cd(Zn)Te and SiO_2 particulates were observed and measured on the (112)B wafer surface by EDS. Thus, we conclude that the particulates measured last year by AFM on the (112)B as-received CdZnTe surface are due to a mixture of residual SiO_2 polishing grit and CdZnTe flakes.

In Fig. 2a, a low-resolution SEM/EDS analysis of the edge of the 6 cm × 6 cm as-received CdZnTe wafer is shown. In Fig. 2b, a high-resolution SEM/

Table II. Results of TXRF analysis of one 6 cm × 6 cm and one 4 cm × 4 cm (112)B CdZnTe wafer subjected to MBE preparation etch

	Al Atoms (cm^{-2})	Si Atoms (cm^{-2})	P Atoms (cm^{-2})	S Atoms (cm^{-2})	Cl Atoms (cm^{-2})	Fe Atoms (cm^{-2})	Cu Atoms (cm^{-2})	Br Atoms (cm^{-2})	Zn Atoms (cm^{-2})	Particles (cm^{-2})
Maximum density, 6 cm × 6 cm wafer	2.36×10^{15}	2.80×10^{13}	9.80×10^{13}	4.30×10^{13}	4.17×10^{13}	7.10×10^{12}	2.17×10^{12}	2.90×10^{14}	1.17×10^{14}	8.00×10^{7}
Average density, 6 cm × 6 cm wafer	5.60×10^{14}	1.37×10^{13}	5.58×10^{13}	2.80×10^{13}	2.38×10^{13}	8.86×10^{11}	1.50×10^{11}	1.63×10^{14}	5.41×10^{13}	3.02×10^{7}
Coefficient of variation, 6 cm × 6 cm wafer	0.90	0.46	0.29	0.23	0.26	1.92	2.81	0.36	0.39	0.94
Skew, 6 cm × 6 cm wafer	3.08	1.19	1.00	0.30	1.27	3.05	4.98	0.43	1.70	0.91
Maximum density, 4 cm × 4 cm wafer	8.50×10^{14}	4.00×10^{13}	9.80×10^{13}	4.40×10^{13}	7.50×10^{13}	1.00×10^{13}	5.20×10^{12}	2.25×10^{13}	1.70×10^{14}	N/A
Average density, 4 cm × 4 cm wafer	4.51×10^{14}	1.74×10^{13}	5.94×10^{13}	2.55×10^{13}	3.93×10^{13}	2.43×10^{12}	4.50×10^{10}	1.78×10^{13}	7.84×10^{13}	N/A
Coefficient of variation, 4 cm × 4 cm wafer	0.40	0.68	0.37	0.33	0.42	1.05	38.19	0.21	0.65	N/A
Skew, 4 cm × 4 cm wafer	0.55	0.94	0.73	1.42	1.63	2.93	3.00	0.44	1.94	N/A

EDS analysis near the bevel edge of the as-received CdZnTe wafer is shown. These two images demonstrate that residual SiO_2 and possibly Al_2O_3 polishing grit as well as residual mounting wax remain on the as-received wafer edge. In Fig. 2c, an SEM/EDS image of a residual Cd(Zn)Te particle left on the wafer edge is shown.

Impurity Analysis of MBE Preparation-Etched Substrates

One 6 cm × 6 cm and one 4 cm × 4 cm state-of-the-art (112)B CdZnTe wafer were MBE preparation etched and analyzed using TXRF. The results from the impurity analysis are presented in Table II. Once again, the elements Cr, Mn, Ni, Ga, Ge, As, Sr, Y, Ta, W, Pt, Au, Hg, Pb, and Bi all had maximum concentrations $\leq 1 \times 10^{12}$ atoms cm^{-2} on the MBE preparation-etched CdZnTe surface and are not shown in the table.

The MBE preparation-etched 6 cm × 6 cm CdZnTe substrate was characterized for surface topography by AFM. Figure 3 shows three AFM images of the MBE preparation-etched 6 cm × 6 cm wafer. The root-mean-square (RMS) roughness of the wafer varied from ~0.5 nm to 1.0 nm across the wafer surface. Particulate length varied from 250 nm to 1 μm. The height of the particulates was measured to be between 10 nm and 50 nm above the (112)B surface. The range of particulate density was 4×10^6 cm^{-2} to 8×10^7 cm^{-2}. Figure 4 shows a map of the particulate density for the MBE preparation-etched 6 cm × 6 cm wafer. There is a factor of 20 variation of particulate density across the 6 cm × 6 cm wafer.

In Fig. 5a and b, high-resolution SEM/EDS analysis of particulates on the 6 cm × 6 cm MBE preparation-etched CdZnTe wafer is shown. Most of the particulates observed on the (112)B surface by SEM/EDS were residual Cd(Zn)Te particles/flakes (some residual C-based particulates were also observed, but these could have been due to MBE preparation etch handling). No residual SiO_2 polishing grit was observed. The SEM/EDS analysis demonstrates that the particulates measured by AFM on the (112)B MBE preparation-etched CdZnTe surface are primarily due to residual CdZnTe particles/flakes.

In Fig. 6a, a low-resolution SEM/EDS analysis of the edge of the MBE preparation-etched 6 cm × 6 cm CdZnTe wafer is shown. In Fig. 6b, a high-resolution SEM/EDS analysis near the bevel edge of the MBE preparation-etched CdZnTe wafer is shown. Residual Cd(Zn)Te particulates were detected by EDS analysis. These two images demonstrate that the residual SiO_2 polishing grit, as well as the residual mounting wax, have been removed from the wafer edge by the MBE preparation etch.

Comparison of Contamination on As-Received and MBE Preparation-Etched Wafers

Figure 7 shows a comparison of the TXRF contamination levels found for the as-received and

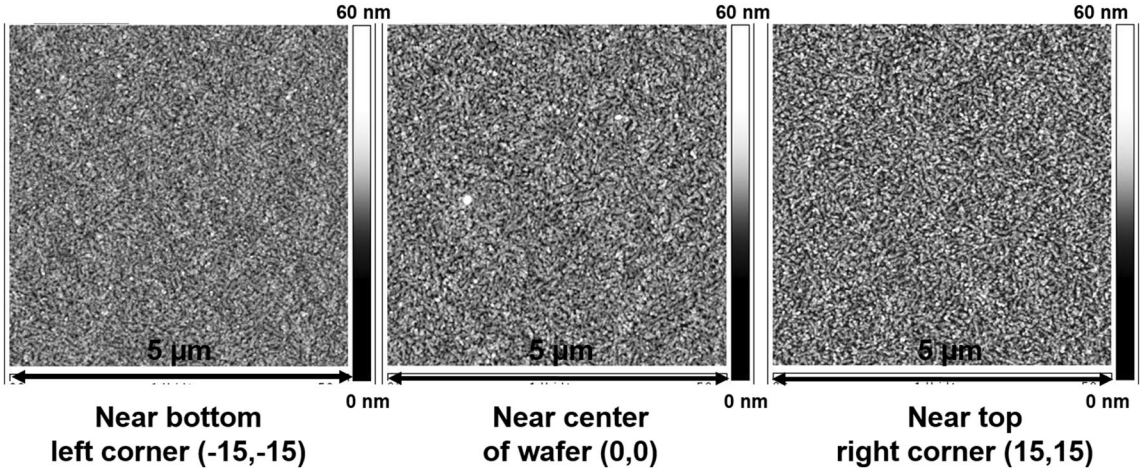

Fig. 3. AFM measurements of MBE preparation-etched 6 cm × 6 cm (112)B Nikko CdZnTe surface.

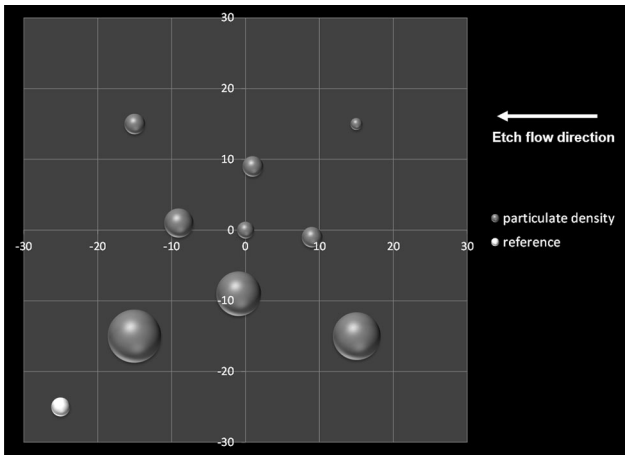

Fig. 4. Graphical representation of AFM measurements of particulate density on MBE preparation-etched 6 cm × 6 cm (112)B CdZnTe wafer. The diameter of the sphere in the figure is proportional to the density of particulates measured. A reference sphere of 1×10^7 cm^{-2} is shown in the bottom-left corner at (−25, −25) mm.

MBE preparation-etched wafers. Overall, the level of contamination for both the as-received and the MBE preparation-etched wafers is very high. The MBE preparation etch leaves undesirable levels of surface contamination for initiation of HgCdTe deposition. The only significant effect of the MBE preparation etch on impurity contamination was to reduce the level of Cl on the wafer surface.

To investigate the correlations in impurity contamination, the Pearson correlation coefficient (with values between +1 and −1, where 1 is total positive correlation, 0 is no correlation, and −1 is total negative correlation) was determined between each pair of impurity elements on each wafer as measured by TXRF. The results are shown in Fig. 8. If two elements' Pearson correlation coefficient is >0.60 for all the samples measured, those elements are said to be correlated. As can be observed from Fig. 8, there is a correlation of the lateral impurity concentration of Si, Cl, P, and S for the as-received substrates. For the MBE preparation-etched substrates, there is a lateral impurity correlation of Cl, P, and S.

DISCUSSION

The analysis of the as-received wafers clearly demonstrates that they are not "epi-ready, out of the box." In the TXRF analyses of the as-received CdZnTe, surface impurity concentrations are well above the level acceptable for standard semiconductor processing.[14] The wide lateral variation (either coefficient of variation >1 or skew >2) in surface contamination of many of the impurities in Table I is also highly problematic. The EDS spectra shown in Figs. 1 and 2 demonstrate that some of the Si contamination found on the as-received CdZnTe substrates in the TXRF analysis comes from residual SiO_2 polishing grit. Al has the highest impurity concentration found in the TXRF analysis of the as-received wafers, as shown in Fig. 7. Colloidal silica polishing slurry can be stabilized with Al. Al was also detected in Fig. 2 in the SEM/EDS analysis. The Al TXRF signal in Fig. 2 could also come from Al_2O_3 polishing grit used to bevel the substrate edge (it is presumed that edge beveling is done prior to final surface polishing). Unfortunately, the orientation required for detecting the wafer edge for SEM/EDS analysis also produced spurious signal from the substrate holder, which is made of Al. This makes confirmation of Al_2O_3 polishing grit problematic. In Fig. 5c, a large piece of carbon-coated Al_2O_3 is observed on the MBE preparation-etched (112)B surface near the wafer edge. Since this particle was detected in plan-view SEM/EDS, no spurious Al signal from the substrate holder interfered with the measurement. This large piece of Al_2O_3 could be residual polishing grit from beveling the wafer edge.

The CdZnTe wafer's surface impurity and damage layer dictate that an MBE preparation etch is

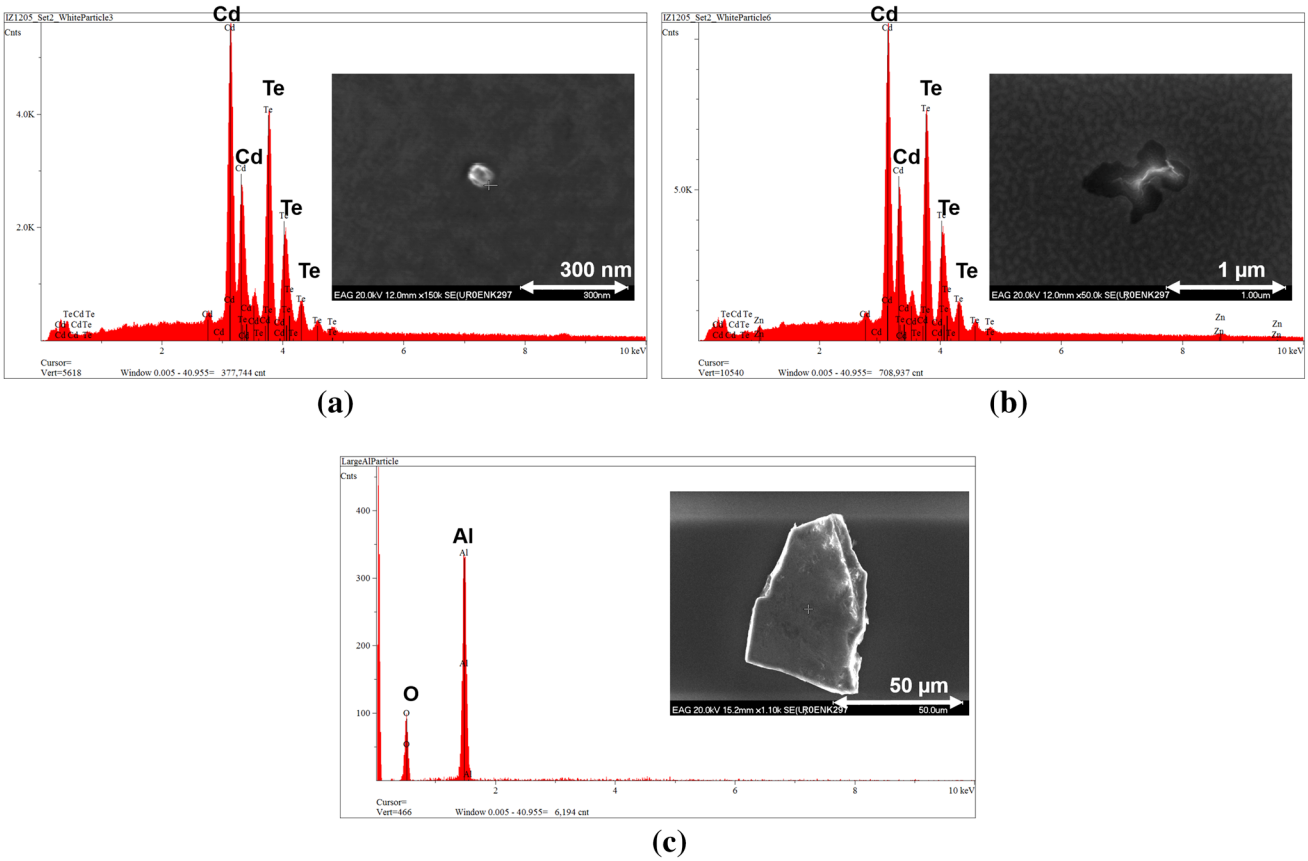

Fig. 5. High-resolution SEM/EDS image analysis of a MBE preparation-etched 6 cm × 6 cm CdZnTe wafer. In (a), one small spherical particulate composed of CdZnTe is shown. In (b), the SEM image shows a flake that EDS determines to be CdZnTe. In (c), the SEM/EDS profile of residual Al_2O_3 left on (112)B surface near the wafer edge is shown.

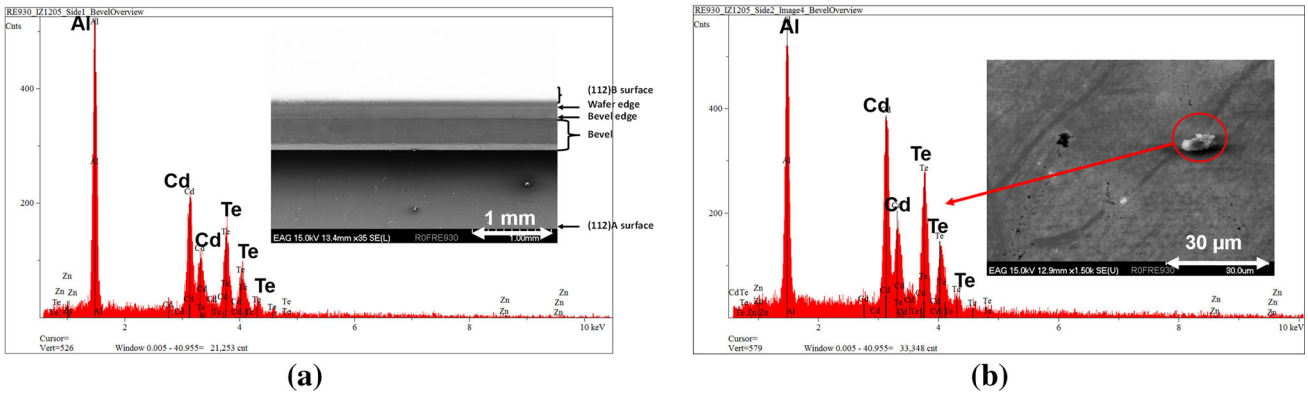

Fig. 6. SEM/EDS image analysis of edge of a MBE preparation-etched CdZnTe wafer: (a) low-resolution image showing the wafer edge, (b) high-resolution image and corresponding EDS profile of Cd(Zn)Te particulate left on the wafer edge.

required. The ultimate goal of the MBE preparation etch technique is to provide a clean, stoichiometric, atomically smooth, and well-ordered surface to minimize growth defects. The high contamination levels, lateral variation in contamination, residual polishing grit, and surface damage of the as-received wafer dictate what the MBE preparation etch needs to eliminate to produce a substrate ready for MBE HgCdTe epitaxial deposition. Unfortunately, as shown in Fig. 7, the current Br:methanol-based MBE preparation etch does not significantly reduce the contamination level. Additionally, the wide lateral variation (either coefficient of variation >1 or skew >2) in surface contamination shown in Table II for many impurities would make uniform HgCdTe processing problematic. These results are

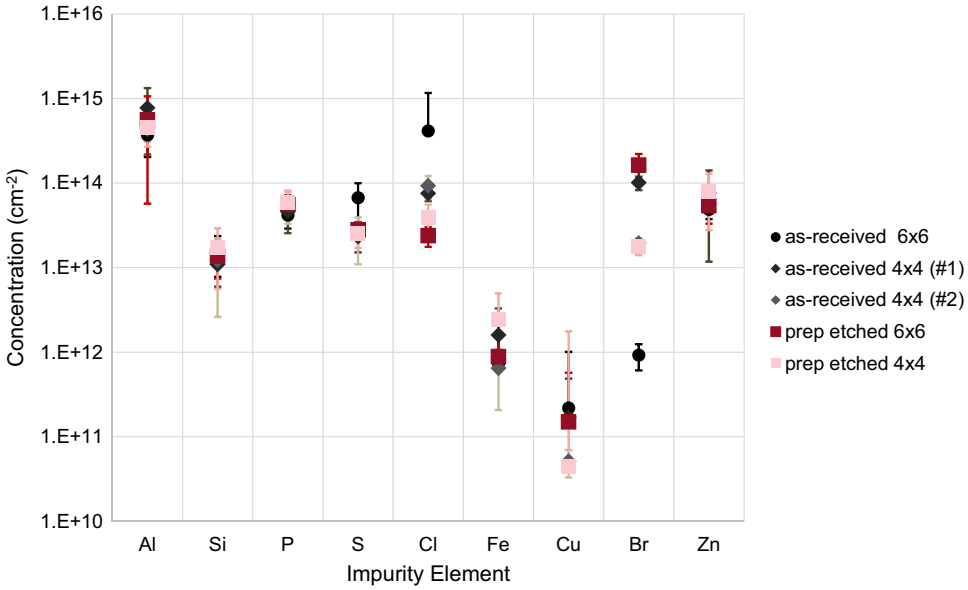

Fig. 7. Graphical representation of TXRF data for as-received and MBE preparation-etched samples.

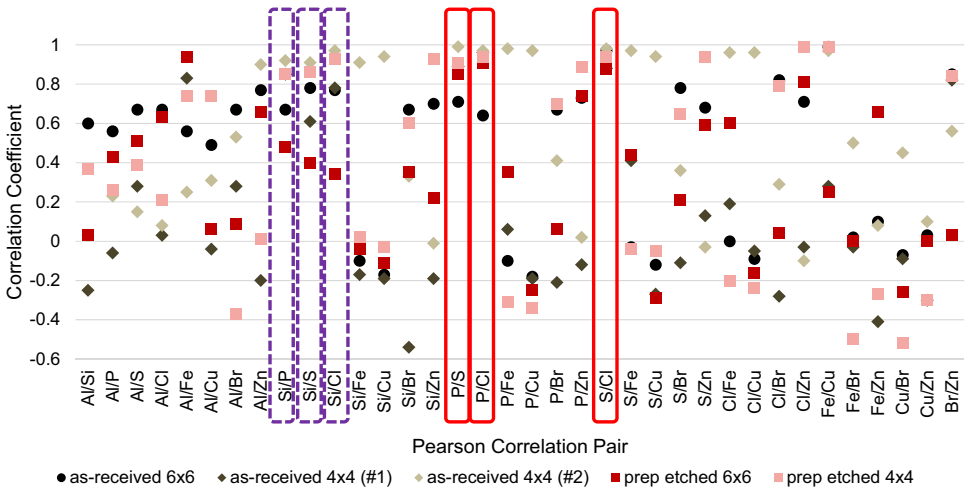

Fig. 8. Graphical representation of Pearson correlation coefficients for as-received and MBE preparation-etched samples. Solid and dashed boxes highlight elements that are correlated (Pearson coefficient >0.60) for the as-received samples measured. Solid boxes highlight elements that are correlated for the MBE preparation-etched samples measured.

not very surprising, since the current Br:methanol-based etch was not designed to reduce surface impurities (especially metallic impurities) as other standard semiconductor cleaning techniques do.[14] The only impurity element measured by TXRF that was reduced below the as-received concentration following the MBE preparation etch was Cl. Cl is highly soluble in the organic solvents used in the MBE preparation etch; this potentially accounts for the reduction in Cl contamination after the MBE preparation etch shown in Fig. 7.

Figures 5 and 6 demonstrate that the MBE preparation etch is capable of removing the SiO_2 polishing grit and wax from the wafer edge and the (112)B wafer surface. The authors speculate that the Br:methanol MBE preparation etch partially solubilizes the SiO_2 polishing grit and disperses trace amounts (below the density which SEM/EDS can easily detect) of residual grit on the wafer surface. This could account for the nearly constant level of Si and Al contamination found in Fig. 7 for as-received and MBE preparation-etched wafers. Further, the authors speculate that the Br:methanol MBE preparation etch also partially solubilizes residual CdZnTe particles left on the as-received wafer surface and edge (shown in Figs. 1b and 2c) and redeposits them on the wafer surface. The redeposition occurs as the CdZnTe wafer is removed from the MBE preparation etch solutions. This could account for the particulate density

pattern (observed in Fig. 4) following the flow pattern left on the wafer surface from the MBE preparation etch.

Finally, the correlation in Fig. 8 of Si, P, Cl, and S for the as-received wafers and P, Cl, and S for the MBE preparation-etched wafers suggests that one of the processes involved in the SiO_2 polishing of the CdZnTe wafers is contaminating the substrates. The authors speculate that the Cl contamination could be due to NaClO, which is used as a standard polishing slurry cleaner. P and S are common components in surfactants used for slurry cleaning solutions.

CONCLUSIONS

As-received Nikko CdZnTe wafers were characterized for polishing residue and impurity contamination. Two 4 cm × 4 cm and one 6 cm × 6 cm (112)B state-of-the-art as-received CdZnTe wafers were analyzed using TXRF. A maximum surface impurity concentration of Al = 1.7×10^{15} atoms cm^{-2}, Si = 3.7×10^{13} atoms cm^{-2}, Cl = 3.12×10^{15} atoms cm^{-2}, S = 1.7×10^{14} atoms cm^{-2}, P = 1.1×10^{14} atoms cm^{-2}, Fe = 1.0×10^{13} atoms cm^{-2}, Br = 1.2×10^{14} atoms cm^{-2}, and Cu = 4×10^{12} atoms cm^{-2} was observed on the as-received CdZnTe wafers. Wide lateral variation (either coefficient of variation >1 or skew >2) in surface contamination for the as-received wafers was observed for many of the above elements. The elements Cr, Mn, Ni, Ga, Ge, As, Sr, Y, Ta, W, Pt, Au, Hg, Pb, and Bi all had concentrations ≤1×10^{12} atoms cm^{-2} on the as-received CdZnTe surface.

As-received wafers were further characterized for polishing residue. The final polishing step leaves residual polishing grit and CdZnTe particles. There was a factor of 7 variation of residual polishing grit/CdZnTe particle density across a 6 cm × 6 cm wafer. SEM/EDS profiles showed the polishing grit on the (112)B surface is composed of SiO_2. Some "large" particulates appear to be agglomerations of smaller pieces of polishing grit. Polishing grit appears to be electrostatically held on the top surface of the CdZnTe. SEM/EDS analysis of the edge of the 6 cm × 6 cm as-received CdZnTe wafer shows that the wafer edge has been beveled. Residual SiO_2 and possibly Al_2O_3 polishing grit, Cd(Zn)Te particles, as well as residual mounting wax remain on the as-received wafer edge.

As-received wafers are not epi-ready "out of the box." The wafers' surface damage and impurity levels dictate that an MBE preparation etch is required. The ultimate goal of the MBE preparation etch technique is to provide a clean, stoichiometric, atomically smooth, and well-ordered surface to minimize growth defects. The current Br:methanol-based MBE preparation etch does not significantly reduce the contamination level of impurities on the surface. A maximum surface impurity contamination of Al = 2.4×10^{15} atoms cm^{-2}, Si = 4.0×10^{13} atoms cm^{-2}, Cl = 7.5×10^{13}atoms cm^{-2}, S = 4.4×10^{13} atoms cm^{-2}, P = 9.8×10^{13} atoms cm^{-2}, Fe = 1.0×10^{13} atoms cm^{-2}, Br = 2.9×10^{14} atoms cm^{-2}, and Cu = 5.2×10^{12}atoms cm^{-2} was observed on the MBE preparation-etched CdZnTe wafers. Additionally, the wide lateral variation (either coefficient of variation >1 or skew >2) in surface contamination for many impurities would make uniform HgCdTe processing problematic. The MBE preparation-etched surface contamination consists of Cd(Zn)Te particles and flakes. No residual SiO_2 polishing grit was observed on the (112)B surface by SEM/EDS analysis. SEM/EDS analysis of the edge of the 6 cm × 6 cm MBE preparation-etched CdZnTe wafer demonstrates that the residual SiO_2 polishing grit, as well as the residual mounting wax, have been removed from the wafer edge by the MBE preparation etch.

REFERENCES

1. M. Reddy, J. Wilde, J.M. Peterson, D.D. Lofgreen, and S.M. Johnson, *J. Electron. Mater.* 41, 2957 (2013).
2. M. Reddy, W.A. Radford, D.D. Lofgreen, K.R. Olsson, J.M. Peterson, and S.M. Johnson, *J. Electron. Mater.* 43, 2991 (2014).
3. M. Reddy, D.D. Lofgreen, K.A. Jones, J.M. Peterson, W.A. Radford, J.D. Benson, and S.M. Johnson, *J. Electron. Mater.* 42, 3114 (2013).
4. J.D. Benson, L.O. Bubulac, M. Jaime-Vasquez, C.M. Lennon, P.J. Smith, R.N. Jacobs, J.K. Markunas, L.A. Almeida, A. Stoltz, J.M. Arias, P.S. Wijewarnasuriya, J. Peterson, M. Reddy, M.F. Vilela, S.M. Johnson, D.D. Lofgreen, A. Yulius, M. Carmody, S. Couture, J. Fiala, and S. Motakef, *J. Electron. Mater.* 44, 3082 (2015).
5. JX Nippon Mining & Metals USA, Inc. (JX Nippon Mining & Metals USA, Inc., 2011), http://www.nikkometals.com/products.html. Accessed 26 Jan 2016.
6. J.D. Benson, A.B. Cornfeld, M. Martinka, K.M. Singley, Z. Derzko, P.J. Shorten, J.H. Dinan, P.R. Boyd, F.C. Wolfgram, B.H. Johs, P. He, and J.A. Wollam, *J. Electron. Mater.* 25, 1406 (1996).
7. M. Zandian, J.M. Arias, J. Bajaj, J.G. Pasko, L.O. Bubulac, and R.E. DeWames, *J. Electron. Mater.* 24, 1207 (1995).
8. C.K. Egan, P. Dabrowski, Z. Klusek, and A.W. Brinkman, *J. Electron. Mater.* 38, 1528 (2009).
9. H. Yoon, J.M. Van Scyoc, M.S. Goorsky, H. Hermon, M. Schieber, J.C. Lund, and R.B. James, *J. Electron. Mater.* 26, 529 (1997).
10. J.N. Johnson, L.A. Almeida, M. Martinka, J.D. Benson, and J.H. Dinan, *J. Electron. Mater.* 28, 817 (1999).
11. P. Moravec, V.G. Ivanits'ka, J. Franc, Z.F. Tomashik, V.M. Tomashik, K. Masek, P.I. Feychuk, L.P. Shcherbak, P. Hoschl, R. Grill, and J. Walter, *J. Electron. Mater.* 38, 1645 (2009).
12. J.D. Benson, L.O. Bubulac, P.J. Smith, R.N. Jacobs, J.K. Markunas, M. Jaime-Vasquez, L.A. Almeida, A. Stoltz, P.S. Wijewarnasuriya, G. Brill, Y. Chen, J. Peterson, M. Reddy, M.F. Vilela, S.M. Johnson, D.D. Lofgreen, A. Yulius, G. Bostrup, M. Carmody, D. Lee, and S. Couture, *J. Electron. Mater.* 43, 3993 (2014).
13. Materials Characterization (Evans Analytical Group, 2016), www.eag.com/mc/total-reflection-x-ray-fluorescence.html. Accessed 26 Jan 2016.
14. W. Kern, *Handbook of Silicon Wafer Cleaning Technology*, ed. K.A. Reinhardt and W. Kern Norwich (New York: William Andrew, 2008), pp. 4–13.